

## Nonlinear dynamic response of a pazy wing variant using Koiter-Newton model reduction

Sinha, Kautuk; Alijani, F.; Krueger, Wolf R. ; De Breuker, R.

**Publication date**

2024

**Document Version**

Final published version

**Published in**

Aeroelasticity & Structural Dynamics in a Fast Changing World 17 – 21 June 2024, The Hague, The Netherlands

**Citation (APA)**

Sinha, K., Alijani, F., Krueger, W. R., & De Breuker, R. (2024). Nonlinear dynamic response of a pazy wing variant using Koiter-Newton model reduction. In *Aeroelasticity & Structural Dynamics in a Fast Changing World 17 – 21 June 2024, The Hague, The Netherlands* Article IFASD 2024-142

**Important note**

To cite this publication, please use the final published version (if applicable). Please check the document version above.

**Copyright**

Other than for strictly personal use, it is not permitted to download, forward or distribute the text or part of it, without the consent of the author(s) and/or copyright holder(s), unless the work is under an open content license such as Creative Commons.

**Takedown policy**

Please contact us and provide details if you believe this document breaches copyrights. We will remove access to the work immediately and investigate your claim.

## NONLINEAR DYNAMIC RESPONSE OF A PAZY WING VARIANT USING THE KOITER-NEWTON MODEL REDUCTION

**Kautuk Sinha<sup>1</sup>, Farbod Alijani<sup>2</sup>, Wolf R. Krueger<sup>1</sup>, Roeland De Breuker<sup>3</sup>**

<sup>1</sup> German Aerospace Center, Institute of Aeroelasticity, Bunsenstrasse 10, 37073, Goettingen, Germany

<sup>2</sup> Delft University of Technology, Faculty of Mechanical Engineering, Mekelweg 2, 2628 CD Delft, Netherlands

<sup>3</sup> Delft University of Technology, Faculty of Aerospace Engineering, Kluyverweg 1, 2629 HS Delft, Netherlands

**Keywords:** Model order reduction, large amplitude motion, flexible wing, nonlinear

**Abstract:** Nonlinear structural analyses in the finite element (FE) framework are often computationally expensive due to their utilization of incremental predictor-corrector solvers. Application of reduced order models for such cases has proven to be beneficial, especially for dynamic loading conditions. Recent developments in the novel Koiter-Newton (K-N) model reduction technique enable us to study large deflection behavior in cantilevered structures. The K-N approach is a reduced basis method which describes a system of nonlinear governing equations comprising quadratic and cubic stiffness terms. The higher order stiffness terms are evaluated as derivatives of the in-plane strain energy. In the case of extremely large deflections, to ensure that the foreshortening effect is accounted for, the reduced order model is updated at fixed load intervals. Linear eigenmodes of the deformed structure are used to formulate the reduction subspace at the different load steps. The objective of this work is to assess the effectiveness of the K-N method with the intended application to a nonlinear benchmark highly flexible wing. Investigations are carried out pertaining to nonlinear static and dynamic characteristics of the wing. Comparisons are made to the solutions from MSC Nastran for verification purpose. The results show that the K-N method requires a significantly small number of degrees-of-freedom to reproduce the Nastran solutions with a marginal loss in accuracy.

### 1 INTRODUCTION

Increasing interest in high aspect ratio (HAR) and flexible wing designs has led the way to structural and aeroelastic investigations of wings in the geometrically nonlinear domain. Early investigations pertaining to high altitude long endurance (HALE) aircraft have demonstrated significant variations in the dynamic characteristics when nonlinearities are included in the analyses [1, 2]. Experimental studies conducted in [3] investigate the nonlinear response analysis of an HAR wing excited by gust loads and it is highlighted that the induced static nonlinearity influences the dynamic characteristic of the wing, thus, also impacts the gust response. More recently in the framework of the Third Aeroelastic Prediction Workshop, Large Deflection Working Group (LDWG), major collaborative efforts have been made to investigate the nonlinear characteristics of the benchmark Pazy wing [4]. The wing has been designed to withstand tip

deflections up to 50 % of the semi-span and thus, serves as an excellent reference model for studying nonlinear effects and validating nonlinear formulations. Some of the early investigations on the nonlinear static and dynamic characteristics of the Pazy wing, presented in [5-8], demonstrate the necessity of incorporating nonlinear analysis techniques in early design stages of highly flexible wings.

While it is evident that large deflections introduce kinematics that linear analyses are incapable of capturing, utilization of nonlinear analyses techniques also implies higher computational times. The generally used predictor-corrector model with incremental loading is the primary causative factor behind the larger computational effort needed in nonlinear analyses. Application of reduced order models (ROMs) have been found to be beneficial in considerably reducing the computational effort, especially in dynamic analyses. A commonly used approach in aircraft design is to develop equivalent beam models which can mimic the structural characteristics of the actual wing [1,6,9,10]. Some researchers have focused on developing eigenmode-based ROMs derived directly from global finite element (FE) models [11-13]. The Koiter-Newton (K-N) reduction method adds to the family of ROMs applicable to generic FE models. The method was initially developed for nonlinear buckling analyses of panel structures [14]. The formulation was then adapted for application to nonlinear dynamic investigations of simple plate structures with various boundary conditions [15]. Large deflection static and dynamic behaviour in cantilevers have been subsequently investigated with the proposition of ROM updating algorithms to account for the cantilever foreshortening effects [16, 17].

The work presented in this article demonstrates the application of the novel developments in the K-N reduction formulation with the Pazy wing as a validation test case. The model is first verified through nonlinear static analysis. Then modal analysis of the deformed wing is conducted and the evolution of eigenfrequencies with increasing nonlinear deflection is shown. For the final test case, the ROM is applied to study the large amplitude dynamic response of the Pazy wing. Comparisons are made to simulations from MSC Nastran in terms of the accuracy and the simulation time. The objective ultimately is to demonstrate the effectiveness of the ROM for the analysis of such nonlinear models. The framework utilized for the ROM-based analyses is entirely developed in Matlab comprising its own FE solver for static, dynamic and eigenmode computations and the necessary modules for ROM generation.

The remainder of the article is organized as follows: Section 2 describes the theoretical formulation of the K-N reduction, Section 3 describes the structural model and its characteristics, the numerical studies are presented in Section 4 and finally, the conclusions of this study are presented in Section 5.

## **2 KOITER-NEWTON MODEL REDUCTION**

This section summarizes the theoretical formulation of the Koiter-Newton model reduction technique. One of the key characteristics of this approach is that it can be applied directly to finite element models. The formulation considers a modified nonlinear governing equation of motion comprising higher order stiffness terms. These higher order stiffness terms are evaluated as derivatives of the in-plane strain energy of the system. The strain energies are based on the nonlinear Green-Lagrange strain formulation and consequently, produces up to third order

stiffness tensors. For conciseness, only the relevant equations are listed in the following subsection. The reader is referred to [14, 15] for detailed derivations of this method.

## 2.1 Theoretical Formulation

The internal forces in a structure are a function of the displacements  $\mathbf{f}_{int} = \mathbf{f}(\mathbf{u})$ . This can be expanded in the Taylor series in the form:

$$\mathbf{f}(\mathbf{u}) = \mathbf{L}\mathbf{u} + \mathbf{Q}\mathbf{u}\mathbf{u} + \mathbf{C}\mathbf{u}\mathbf{u}\mathbf{u} + O(\|\mathbf{u}\|^4) \quad (1)$$

where  $\mathbf{L}$ ,  $\mathbf{Q}$ ,  $\mathbf{C}$  are the linear, quadratic and cubic stiffness tensors, respectively. The third order governing equation of motion forms the basis of the nonlinear formulation. It is assumed that a linear subspace of the external applied force exists and can be parametrized by coordinates  $\boldsymbol{\phi}$  along the predefined force vectors. The force subspace can be then described as:

$$\mathbf{f} = \mathbf{F}\boldsymbol{\phi} \quad (2)$$

Where  $\mathbf{F}$  consists of the external force vector, along with  $m$  additional perturbation load vectors in the presence of buckling. When post-buckling behavior is not of interest, consideration of the external force vector suffices.

The equilibrium solution of Equation (1) can be parametrized in terms of generalized displacements  $\boldsymbol{\xi}$ .

$$\mathbf{u} = \mathbf{u}_\alpha \boldsymbol{\xi} + \mathbf{u}_{\alpha\beta} \boldsymbol{\xi}\boldsymbol{\xi} + \mathbf{u}_{\alpha\beta\gamma} \boldsymbol{\xi}\boldsymbol{\xi}\boldsymbol{\xi} + O(\|\mathbf{u}\|^4) \quad (3)$$

where  $\alpha, \beta, \gamma$  vary from  $1, 2, \dots, m+1$ .

The parameterization in Equation (3) can be done in infinite ways and therefore, to fix the parameterization  $\boldsymbol{\xi}$  is chosen such that it is a work conjugate to the load amplitudes  $\boldsymbol{\phi}$ , resulting in the equation:

$$(\mathbf{F}\boldsymbol{\phi})' \delta\mathbf{u} = \boldsymbol{\phi}' \delta\boldsymbol{\xi} \quad (4)$$

where the superscript prime indicates transpose.

The load amplitude  $\boldsymbol{\phi}$  is expanded consistent with the displacement expansion as:

$$\boldsymbol{\phi} = \bar{\mathbf{L}}\boldsymbol{\xi} + \bar{\mathbf{Q}}\boldsymbol{\xi}\boldsymbol{\xi} + \bar{\mathbf{C}}\boldsymbol{\xi}\boldsymbol{\xi}\boldsymbol{\xi} + O(\|\boldsymbol{\xi}\|^4) \quad (5)$$

where  $\bar{\mathbf{L}}$ ,  $\bar{\mathbf{Q}}$ ,  $\bar{\mathbf{C}}$  are the unknown ROM variables.

We then substitute the Equations (3) and (5) into (1) and solve for the coefficients of the  $\boldsymbol{\xi}$  terms. Additionally, Equation (3) is substituted into (4) to obtain a set of constraint equations. Together these form the set of equations required for obtaining the ROM parameters.

$$\begin{bmatrix} \mathbf{L} & -\mathbf{F} \\ -\mathbf{F}' & \mathbf{0} \end{bmatrix} \begin{Bmatrix} \mathbf{u}_\alpha \\ \bar{\mathbf{L}}_\alpha \end{Bmatrix} = \begin{Bmatrix} \mathbf{0} \\ -\mathbf{E}_\alpha \end{Bmatrix} \quad (6)$$

$$\begin{bmatrix} \mathbf{L} & -\mathbf{F} \\ -\mathbf{F}' & \mathbf{0} \end{bmatrix} \begin{Bmatrix} \mathbf{u}_{\alpha\beta} \\ \bar{\mathbf{Q}}_{\alpha\beta} \end{Bmatrix} = \begin{Bmatrix} -\mathbf{Q}(\mathbf{u}_\alpha, \mathbf{u}_\beta) \\ \mathbf{0} \end{Bmatrix} \quad (7)$$

$$\bar{\mathbf{C}}_{\alpha\beta\gamma\delta} = \mathbf{C}(\mathbf{u}_\alpha, \mathbf{u}_\beta, \mathbf{u}_\gamma, \mathbf{u}_\delta) - \frac{2}{3} [\mathbf{u}'_{\alpha\beta} \mathbf{L} \mathbf{u}_{\delta\gamma} + \mathbf{u}'_{\beta\gamma} \mathbf{L} \mathbf{u}_{\delta\alpha} + \mathbf{u}'_{\gamma\alpha} \mathbf{L} \mathbf{u}_{\delta\beta}] \quad (8)$$

It is important to highlight here that the formulation presented above is intended for the nonlinear statics problem. Recall that the reduction subspace comprises force vectors. In [16] it has been shown that only the external force vector in the reduction subspace is sufficient to model the static large deflection behavior without considerations of structural instabilities.

The ROM formulation for dynamics diverges to some extent from the above presented theory. Instead of utilizing the external force vector in the reduction subspace, a momentum subspace is utilized for this formulation. It has been shown in [15] that the momentum subspace approach results in a system of equations perfectly analogous to Equations 6-8 and thus, it is possible to utilize the same ROM formulation. Interestingly, the momentum subspace-based ROM also holds validity for nonlinear static analyses. The benefit of adopting the momentum subspace is that it enables easy computation of the reduced mass and reduced damping matrices which so far have not been described. Similar to Equation (2), it is assumed that the momentum subspace  $\mathbf{p}$  is parameterized by coordinates  $\boldsymbol{\pi}$ , as:

$$\mathbf{p} = \mathbf{P}\boldsymbol{\pi} \quad (9)$$

where  $\mathbf{P}$  is the basis matrix for the model reduction and comprises the product of the mass matrix and a modal matrix  $\Phi$  with selected eigenmodes. In this case,  $\mathbf{P}$  replaces the variable  $\mathbf{F}$  in the equations (6)-(7). All other parameters remain same in the equations (6)-(8).

The reduced mass matrix  $\bar{\mathbf{M}}$  can be then identified as:

$$\bar{\mathbf{M}} = \Phi' \mathbf{M} \Phi^{-1} \quad (10)$$

Furthermore, the reduced damping matrix is derived as:

$$\bar{\mathbf{D}} = \bar{\mathbf{M}} (\mathbf{P}' \mathbf{M}^{-1} \mathbf{D} \mathbf{M}^{-1} \mathbf{P}) \bar{\mathbf{M}} \quad (11)$$

where  $\mathbf{M}$  is the mass matrix and  $\mathbf{D}$  is the damping matrix in the full FE model.

The equation of dynamics in the reduced subspace can be then expressed as:

$$\bar{\mathbf{M}} \ddot{\boldsymbol{\xi}} + \bar{\mathbf{D}} \dot{\boldsymbol{\xi}} + \bar{\mathbf{L}} \boldsymbol{\xi} + \bar{\mathbf{Q}} \boldsymbol{\xi} \boldsymbol{\xi} + \bar{\mathbf{C}} \boldsymbol{\xi} \boldsymbol{\xi} \boldsymbol{\xi} = \boldsymbol{\phi}(t) \quad (12)$$

with  $\boldsymbol{\phi} = \mathbf{u}'_\alpha \mathbf{f}_{ext}$ .

For application to general structural models, the required input parameters from the full FE model are the mass matrix, damping matrix, stiffness tensors (including higher order) and the external force vector. Excluding the higher order stiffness terms, these matrices are in general obtainable from any FE code. The higher order stiffness tensors can be obtained as numerical derivatives of element strain energies. This has been previously done in combination with MSC Nastran in [11]. In this work, however, we choose a different approach of obtaining the stiffness terms. The FE solver has been independently developed in Matlab and contains a 6-degree of freedom (DOF) planar beam element along with an 18-DOF triangular shell element [18,19]. This implies that the availability of shape functions of the elements could be exploited in order to obtain the expressions of strain energy in variable form. The derivations of the higher order stiffness tensors from the FE formulations is described in detail in [14, 15]. For completeness, the relevant equations are provided in the Appendix.

## 2.2 Solution methodology

The K-N reduction method has been tested with several boundary conditions. In the case of clamped-clamped structure with stretching induced non-linearity, the ROM performs effectively for a high degree of nonlinearity. Analyzing cantilevers was found to be more challenging. The inherent kinematics of cantilevers limits the validity of the ROM such that it could only be accurate in the domain of moderate geometric nonlinearity. This occurs due to the large rotations and the corresponding foreshortening effect which was originally not accounted for in the ROM formulations. An algorithm was proposed in [16] where the ROM is updated at fixed load intervals such that the region of validity is expanded. The flowchart in Figure 1 is representative of the process flow in the ROM update algorithm in statics.

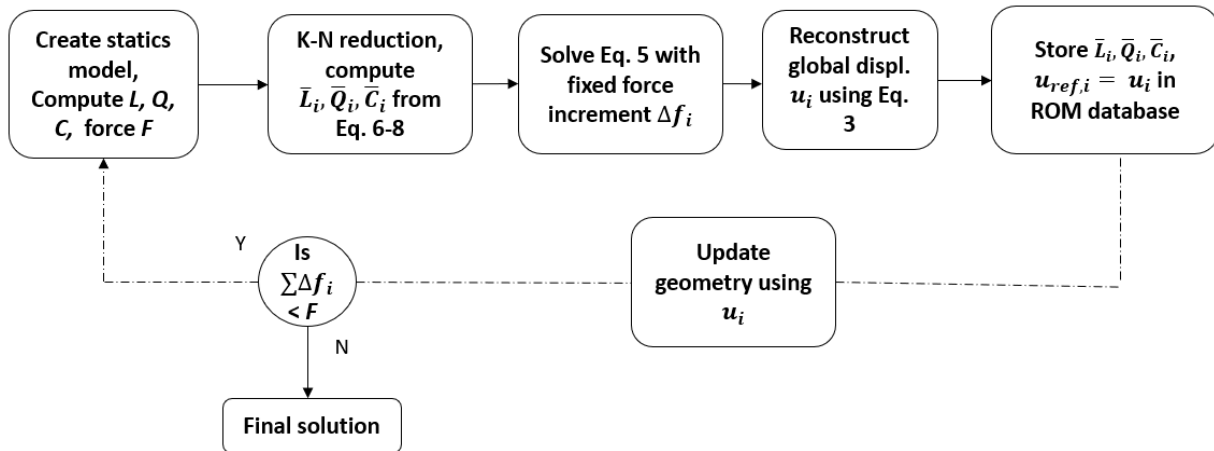


Figure 1: Process flow diagram with ROM updating in nonlinear statics solution

The solution of Equation 5 is executed in the ROM subspace using Newton-Raphson iterations. In the special case, when the reduction subspace is formulated using only the external force vector,

the ROM variables have the size of a 1-DOF system. Thus, we only need to solve an algebraic equation of the third order.

The nonlinear dynamic response is obtained by solving Equation 12. The Newmark beta method [20] for time integration is utilized for this purpose. In this work, the transient response is limited to tip deflections in the neighborhood of 30 % of the wing span. Thus, in this case the ROM is formulated only once in the initial undeformed state. Equations 5 and 12 provide the generalized displacements in the reduced subspace. The actual displacements are obtained through Equation 3. The results of the numerical studies are presented in the subsequent sections.

### 3 STRUCTURAL MODEL

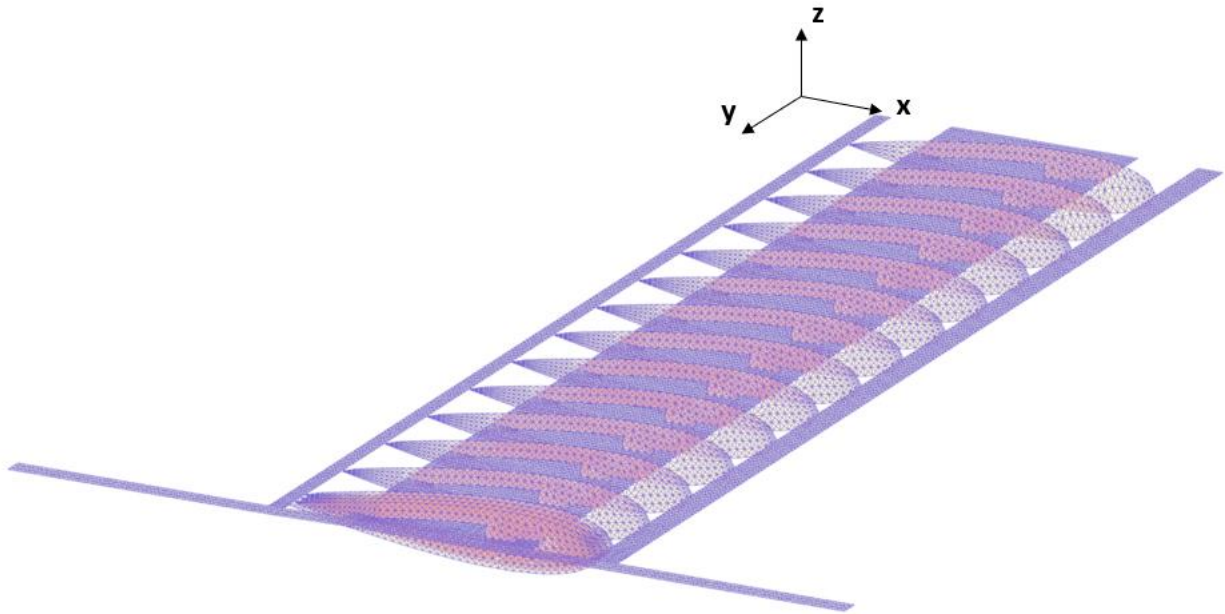


Figure 3: Finite element model of the Pazy wing variant

The FE model utilized in this work, see Figure 3, has been reconstructed based on the approximate dimensions and properties of the Pazy wing [4]. The primary modification in this model is that it is entirely built using shell elements. This adaptation was necessary in order to be able to import the FE model into the Matlab based ROM generation framework which is currently coupled to two FE members (planar beam and triangular shell). In comparison, the original Pazy wing FE model comprises a combination of shell, beam and rigid body elements. Another notable point is that the skin surface is excluded from this model. In [5] it has been discussed that the skin surface in the actual experimental model of the Pazy wing is an *Oralight* plastic film. In the previously conducted FE analyses, this thin surface of the plastic film exhibits strong buckling behavior even at low loads, thus, resulting in severe convergence difficulties in the nonlinear analyses.

The wing spans across 0.56 m, has chord length of 0.11 m and the cross-section is modelled using the NACA0018 airfoil dimensions. The central rectangular plate structure, as seen in Figure 3, is made of Aluminum 7075 while the surrounding frame structure including the airfoil geometry is

made of Nylon 12. Overall, the model consists of 39,930 elements and 21,712 grid points. Due to the modelling adaptations, some obvious differences in the structural characteristics of the original Pazy wing FE model are expected. A modal analysis is conducted to verify the model properties. Table 1 shows a comparison of linear eigenfrequencies of the reference wing model [4], Nastran SOL 103 analysis of the Pazy wing variant and the eigenvalue analysis in the Matlab framework. The results indicate that the presently used shell element model is, in general, less stiff in comparison to the reference model. This can be attributed to the different element types used and the finer meshing in the model. Nevertheless, the shell model is suitable for the investigations conducted in this work. Furthermore, the eigenvalue analyses conducted on the imported FE model in Matlab affirms the successful model import into the Matlab framework.

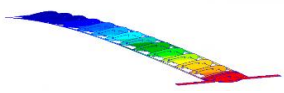
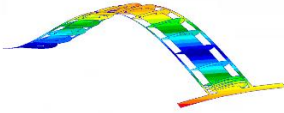
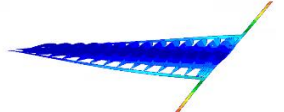
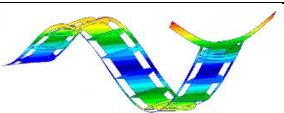
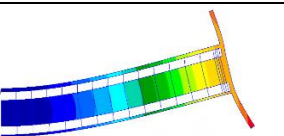
Mode number	Mode Shape	Reference model Nastran SOL 103 [Hz]	Current model Nastran SOL 103 [Hz]	Current model Matlab [Hz]
1		4.42	4.28	4.28
2		28.98	28.12	28.15
3		40.33	38.49	39.47
4		82.40	80.17	80.39
5		112.26	111.5	111.75

Table 1: Comparison of eigenfrequencies of the reference [4] and current models

## 4 RESULTS

This section presents the results of the nonlinear analyses of the Pazy wing. First, initial verification of the nonlinear formulation is done through nonlinear static analyses in Section 4.1. Then, the variation of the eigenfrequencies with large deflections is studied in Section 4.2. Finally, the wing is excited by a dynamic load and the time history of the wing is presented in Section 4.3. Comparisons are made, where applicable, to the corresponding results obtained from MSC Nastran.



#### 4.1 Large deflection static response

The Pazy wing has been designed for tip deflections up to 50 % of the span. As an initial test of the K-N reduction method, we analyze the large deflection behavior of the wing. In addition to the geometric nonlinearity, follower forces are considered i.e. the applied force always remain normal to the surface. The wing is clamped on one end along the  $y = 0$  edge and a tip force of 20 N is applied on the other end at the chordwise central location. Figure 4 compares the nonlinear static deflection along the leading edge of the wing obtained through MSC Nastran and through the K-N reduction method.

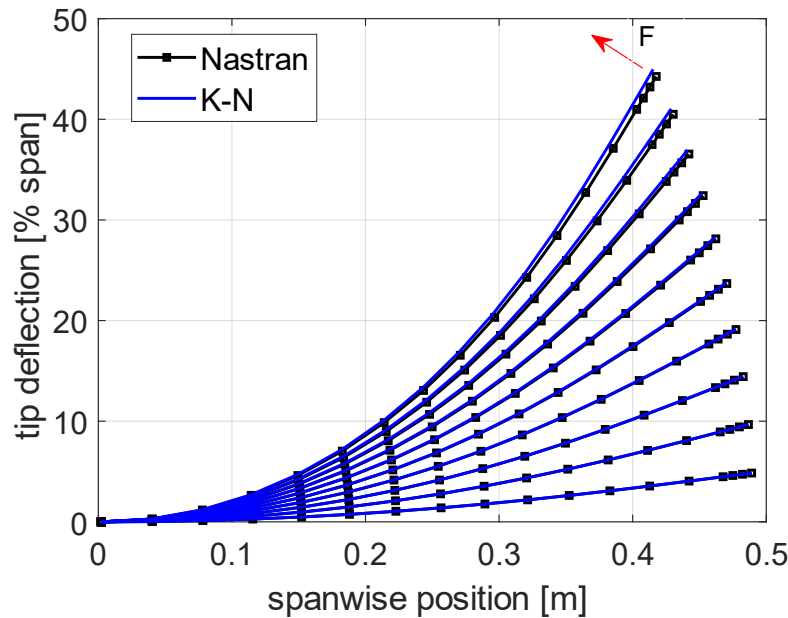


Figure 4: Deflection at the leading edge of the wing with 20 N applied follower force, comparison between Nastran and K-N reduction

The Nastran analyses have been conducted in the SOL 400 module with adaptive load step increment and convergence is based on the internal force and total work done. For the K-N reduction, the external force vector is chosen in the reduction subspace. This creates a 1-DOF reduced order model for each load increment that needs to be solved to obtain the nonlinear solution. In Figure 4, it can be observed that the tip deflection reaches almost 45 % of the span for the applied load. The two analyses show very agreeable results with a difference of only 0.7 % when the maximum tip deflection at 20 N is reached. The total simulation time required to solve for the maximum load of 20 N in Nastran is 96 mins. In total, 626 load increments were needed along with 3152 iterations in the corrector steps. The K-N reduction process is fully executed in about 30 mins with 12 load increments. This includes the pre-processing time (17.5 mins) required for the ROM generation. It is notable that the ROM generation is a one-time process and for any

generic load case it is possible to store the relevant data and reuse it. This implies that when repeated analyses are needed, the simulation time for the ROM is further reduced by at least 50 %.

Next, we conduct a convergence analysis to study the effect of the number of load increments on the ROM solution. Figure 5 depicts the variation in the maximum tip deflection with number of load increments applied for the above described 20 N load case. The convergence plots show that the solution is fully converged at around 20 load increments and a computation time of 48 mins. However, at 12 load increments, the difference from the converged solution is only about 0.03 %.

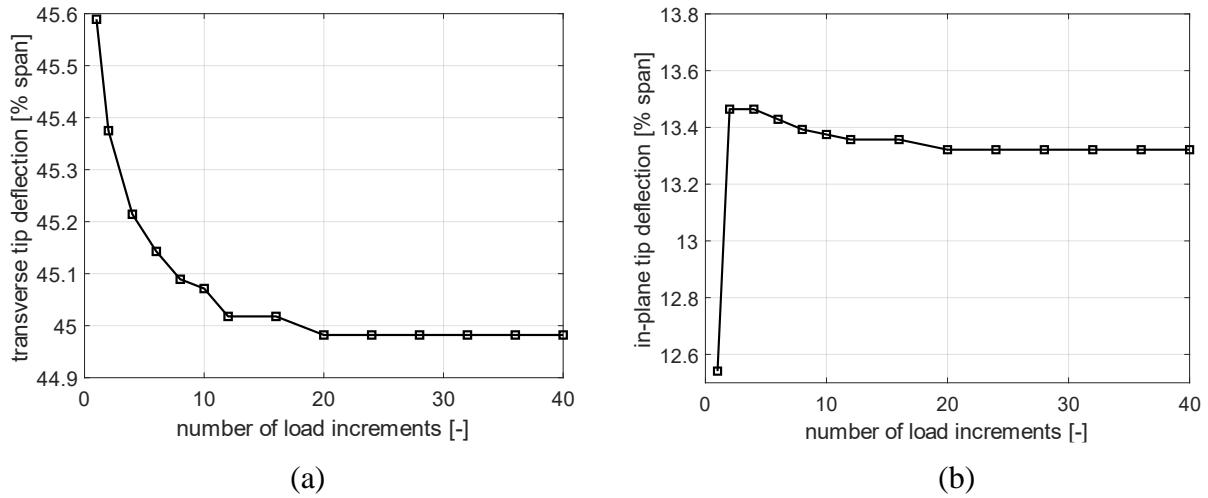


Figure 5: Convergence of transverse (a) and in-plane (b) tip deflections with increasing number of load increments

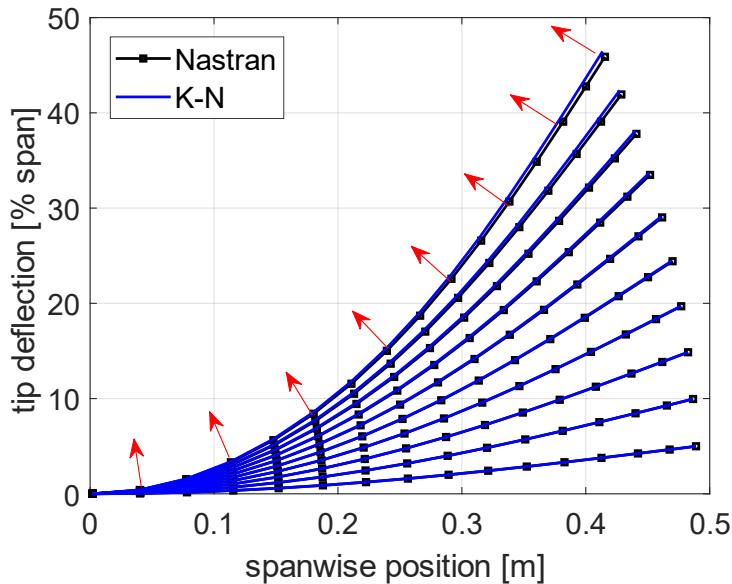


Figure 6: Deflection at the leading edge of the wing with distributed follower force (6 N at each node point), comparison between Nastran and K-N reduction

In general, the ROM can be derived with various loading conditions and is not limited to concentrated single point force. An example is shown in Figure 6 where forces are acting at multiple node points along the wing span. 6 N force is applied at each of the grid points which are located along every alternate rib at the chordwise center position. In this case, the tip deflection obtained from the ROM differs by 1.25 % in comparison to the Nastran solution at maximum loading.

## 4.2 Influence of nonlinearities on eigenfrequencies

In earlier works [5,6] it has been demonstrated that when the deformations of the structure are in the nonlinear domain, there may be significant shifts in the eigenfrequencies. This is expected since the structural stiffness is known to vary in states of large deformation and large strain. Figure 7 depicts the variation of eigenfrequencies with increasing tip deflections (% span). The first five eigenfrequencies obtained from the K-N reduction process are plotted and compared to corresponding results from Nastran. The modes in Figure 6 are abbreviated as OOP (out-of-plane bending), T (torsion) and IP (in-plane bending). The two simulations produce qualitatively very similar results. In Figure 6 it can be observed that the variations in eigenfrequencies, particularly of T1 and IP1, may lead to potential mode couplings with OOP2 and OOP3, respectively.

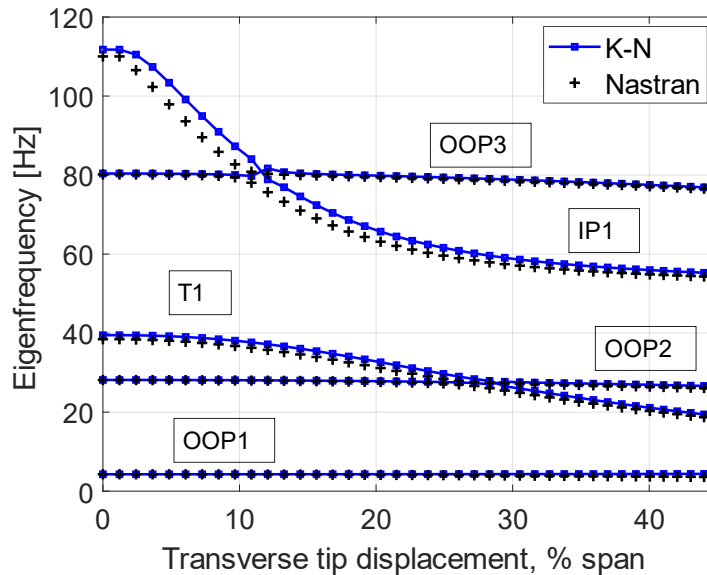


Figure 7: Variation of eigenfrequencies with increasing geometrically nonlinear tip deflection

## 4.3 Dynamic response

The nonlinear dynamic response of the wing is analyzed when subjected to a transient loading. The wing is excited by a concentrated, non-follower, tip force of 4 N that varies as a 1-cosine function of time for one full time period ( $T = 0.233$  sec) and subsequently becomes zero. The excitation frequency is 4.28 Hz. A proportional damping is applied with a damping ratio of 0.093. The relatively large damping ratio had to be chosen since solution convergence in Nastran could

not be achieved at lower damping values. No issues are seen in the ROM solution even at lower damping ratios. The model is simulated for 1.5 sec with a time step of 0.001 sec. In Nastran, adaptive time step increment is utilized with a force and work-based convergence criteria while the ROM utilizes a fixed time step increment. Time history of the wing tip is plotted in Figure 8 and a comparison is made between the ROM and the Nastran nonlinear results. In-plane displacement in Figure 8 refers to the y-direction and the transverse displacement refers to the z-direction of the coordinate system shown in Figure 3.

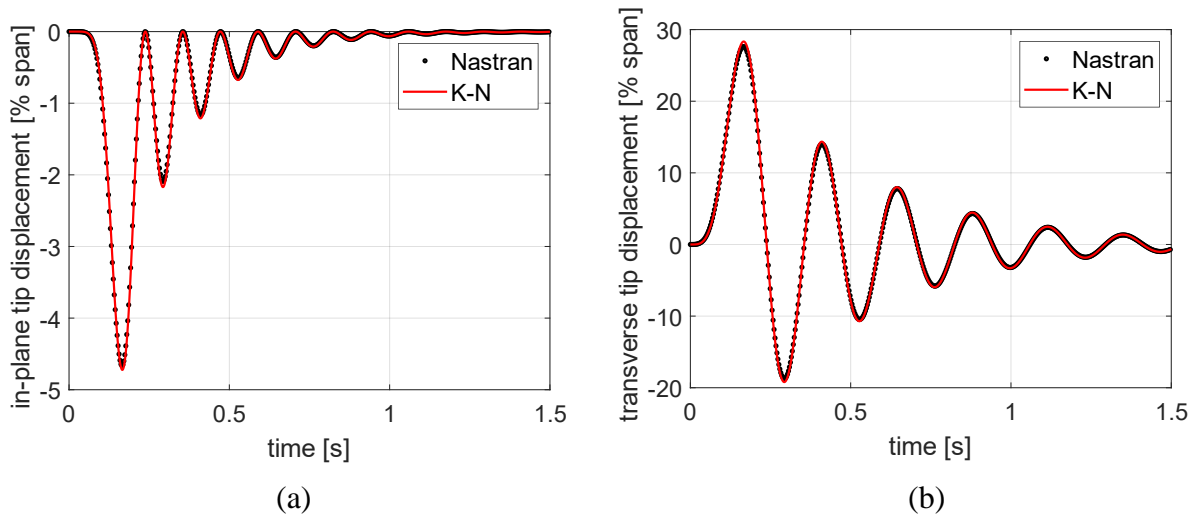


Figure 8: Transient response at the wing tip when subjected to one cycle of a 1-cosine load (a) in-plane displacement (b) transverse displacement

The ROM results agree well with the corresponding Nastran solutions. The maximum transverse displacement in Nastran is estimated at 27.63 % of the span while the ROM predicts 28.3 % of the span. The in-plane displacement is at -4.66 % in Nastran and -4.72 % in Nastran. The total computational time required in Nastran is 4.2 hours. The momentum subspace is now used for the ROM formulation and solution is obtained by utilizing a 2-DOF model. This implies that only the first two eigenmode shapes are used in the reduction subspace. The total time needed for the generation of the ROM parameters is about 33 mins. In addition, just 7.9 secs are needed for computing the transient response from the ROM parameters. The utilization of the ROM is clearly hugely beneficial in improving the analysis efficiency. Evidently, the bulk of the time in the ROM analysis goes into the generation of the ROM. If repeated analyses are to be conducted, it is significantly more beneficial to store the ROM data and reuse it. All simulations have been done on a Linux system with an Intel(R) Xeon(R) W-1290P CPU @ 3.70GHz processor and 132Gb RAM.

Next, we conduct a convergence analysis to demonstrate the influence of the number of modes in the reduction subspace on the solution. Five variations of the ROM are generated using up to the 6<sup>th</sup> eigenmode. The reduction subspace is varied with eigenmode combinations of [1], [1,2], [1,2,3], [1,2,3,4], and [1,2,3,4,6]. The inclusion of the 5<sup>th</sup> eigenmode (in-plane bending) in the reduction subspace was found to cause convergence problems in the dynamic analysis and thus, was excluded. Figure 9 depicts a comparison of the superimposed solutions for all the considered

models (1- to 5-DOF). It can be seen that the 1-DOF model produces a slightly stiffer response with the amplitudes lower by around 0.3 %. The solutions for 2-to 5-DOF models produce very similar responses with negligibly small differences. Thus, the 2-DOF model is found to be sufficient for the present analysis.

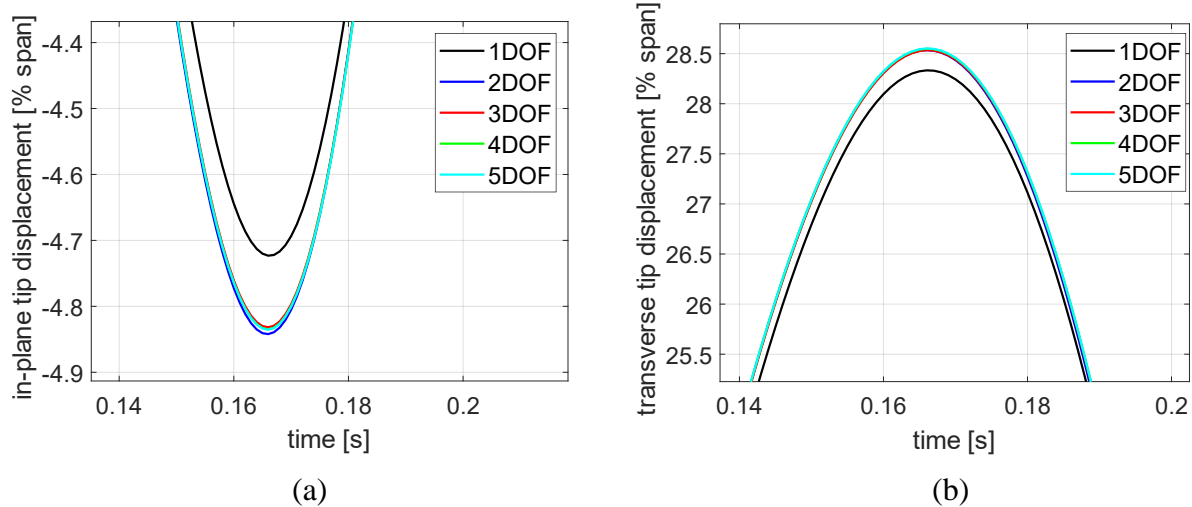


Figure 9: Convergence of solution with increasing number of modes in the reduction subspace (a) in-plane displacement, (b) transverse displacement

## 5 CONCLUSIONS

The nonlinear benchmark Pazy wing is studied in this work using the K-N reduction approach. Recent developments in the K-N reduction approach with respect to modelling of cantilevers have been applied and validated. Comparisons to simulation results from Nastran show that the K-N method is capable of accurately reproducing the deflection behavior in static and dynamic analyses. Convergence analysis has been done in the static case which shows that 12 load increments are sufficient to model large deflection for the Pazy wing. In the dynamic analysis, convergence behavior is studied with respect to the number of modes in the reduction subspace. It is seen that solution quickly converges as we increase the number of modes from 1 to 5. The computation time required is reduced by 68 % in static analysis and 87 % in dynamic analysis including the ROM generation time. Overall, the K-N method performed highly efficiently for the studied test cases and the margin of error in comparison to reference solutions was found to be in an acceptable limit.

## COPYRIGHT STATEMENT

The authors confirm that they, and/or their company or organisation, hold copyright on all of the original material included in this paper. The authors also confirm that they have obtained permission from the copyright holder of any third-party material included in this paper to publish it as part of their paper. The authors confirm that they give permission, or have obtained permission from the copyright holder of this paper, for the publication and public distribution of this paper as part of the IFASD 2024 proceedings or as individual off-prints from the proceedings.

## APPENDIX

Higher order stiffness terms are derived from the strain energy formulations. Triangular shell elements developed in [18, 19] are utilized. Detailed expressions can be found in [14,15].

Total strain in a deformed state  $\mathbf{q}$  is defined as:

$$\varepsilon = \varepsilon_l + \varepsilon_{nl} = (\mathbf{B}_1 + \frac{1}{2} \mathbf{B}_{nl}(\mathbf{q}))\mathbf{q}$$

$$\mathbf{B}_1 = \frac{1}{2A} [\mathbf{B}_1 \ \mathbf{B}_2 \ \mathbf{B}_3],$$

where  $A$  is the element area.

Considering that the three nodal coordinates are  $(x_1, y_1)$ ,  $(x_2, y_2)$  and  $(x_3, y_3)$ ,

$$x_{ij} = x_i - x_j$$

$$y_{ij} = y_i - y_j$$

$$\mathbf{B}_1 = \begin{bmatrix} y_{23} & 0 & 0 & 0 & 0 & \frac{y_{23}(y_{13} - y_{21})}{6} \\ 0 & x_{23} & 0 & 0 & 0 & \frac{x_{32}(x_{32} - x_{12})}{6} \\ x_{32} & y_{32} & 0 & 0 & 0 & \frac{x_{31}y_{13} - x_{12}y_{21}}{3} \end{bmatrix}$$

$$\mathbf{B}_2 = \begin{bmatrix} y_{31} & 0 & 0 & 0 & 0 & \frac{y_{31}(y_{21} - y_{32})}{6} \\ 0 & x_{13} & 0 & 0 & 0 & \frac{x_{13}(x_{12} - x_{23})}{6} \\ x_{13} & y_{31} & 0 & 0 & 0 & \frac{x_{12}y_{21} - x_{23}y_{32}}{3} \end{bmatrix}$$

$$\mathbf{B}_3 = \begin{bmatrix} y_{12} & 0 & 0 & 0 & 0 & \frac{y_{12}(y_{32} - y_{13})}{6} \\ 0 & x_{21} & 0 & 0 & 0 & \frac{x_{21}(x_{23} - x_{31})}{6} \\ x_{21} & y_{12} & 0 & 0 & 0 & \frac{x_{23}y_{32} - x_{31}y_{13}}{3} \end{bmatrix}$$

The nonlinear strain component can be computed using the  $\mathbf{B}_{nl}(\mathbf{q})$  term which is given by:

$$\mathbf{B}_{nl}(\mathbf{q}) = \begin{bmatrix} \mathbf{q}^t \mathbf{K}_{xx} \\ \mathbf{q}^t \mathbf{K}_{yy} \\ \mathbf{q}^t \mathbf{K}_{xy} \end{bmatrix}$$

$$\mathbf{K}_{xx} = \mathbf{B}_w^t \mathbf{T}_x^t \mathbf{T}_x \mathbf{B}_w + \mathbf{B}_v^t \mathbf{T}_x^t \mathbf{T}_x \mathbf{B}_v$$

$$\mathbf{K}_{yy} = \mathbf{B}_w^t \mathbf{T}_y^t \mathbf{T}_y \mathbf{B}_w + \mathbf{B}_u^t \mathbf{T}_y^t \mathbf{T}_y \mathbf{B}_u$$

$$\mathbf{K}_{xy} = \mathbf{B}_w^t (\mathbf{T}_x^t \mathbf{T}_y + \mathbf{T}_y^t \mathbf{T}_x) \mathbf{B}_w$$

Here,

$$\mathbf{T}_x = \frac{1}{2A} [\gamma_{23} \gamma_{31} \gamma_{12}] \quad \text{and} \quad \mathbf{T}_y = \frac{1}{2A} [x_{32} \gamma_{13} x_{21}]$$

The other symbols  $\mathbf{B}_u$ ,  $\mathbf{B}_v$ ,  $\mathbf{B}_w$  represent 3 x 18 matrices. In  $\mathbf{B}_u$  the terms at (1,1), (2,7), and (3,13) are 1 and all other terms are zero. In  $\mathbf{B}_v$  the terms at (1,2), (2,8), and (3,14) are 1 and all other terms are zero. Similarly, in  $\mathbf{B}_w$  the terms at (1,3), (2,9), and (3,15) are 1 and all other terms are zero.

The internal force  $\mathbf{f}$ , tangent stiffness  $\mathbf{L}$ , quadratic stiffness  $\mathbf{Q}$  and cubic stiffness  $\mathbf{C}$  are derived as derivatives of the strain energy with respect to the displacement.

$$\mathbf{f} = A(\mathbf{B}_l' \mathbf{N}_{nl} + \mathbf{B}_{nl}' \mathbf{N})$$

$$\mathbf{L} = A(\mathbf{B}_l' \mathbf{A}_m \mathbf{B}_{nl} + \mathbf{B}_{nl}' \mathbf{A}_m \mathbf{B}_l + \mathbf{B}_{nl}' \mathbf{A}_m \mathbf{B}_{nl} + N_x \mathbf{K}_{xx} + N_y \mathbf{K}_{yy} + N_{xy} \mathbf{K}_{xy})$$

$$\mathbf{N} = \mathbf{N}_l + \mathbf{N}_{nl} = \mathbf{A}_m \mathbf{B}_l \mathbf{q} + \frac{1}{2} \mathbf{A}_m \mathbf{B}_{nl}(\mathbf{q}) \mathbf{q}$$

$$\mathbf{Q}(\mathbf{u}_\alpha, \mathbf{u}_\beta) = \frac{A}{2} (\mathbf{B}_{nl}'(\mathbf{u}_\beta) \mathbf{A}_m \mathbf{B}(\mathbf{u}_\alpha) \mathbf{u}_\alpha + \mathbf{B}_{nl}'(\mathbf{u}_\alpha) \mathbf{A}_m \mathbf{B}(\mathbf{u}_\beta) \mathbf{u}_\beta + \mathbf{B}' \mathbf{A}_m \mathbf{B}_{nl}(\mathbf{u}_\alpha) \mathbf{u}_\beta)$$

$$\begin{aligned} \mathbf{C}(\mathbf{u}_\alpha, \mathbf{u}_\beta, \mathbf{u}_\gamma, \mathbf{u}_\delta) &= \frac{A}{6} (\mathbf{A}_m \mathbf{B}_{nl}(\mathbf{u}_\alpha) \mathbf{u}_\delta \mathbf{B}_{nl}(\mathbf{u}_\beta) \mathbf{u}_\gamma + \mathbf{A}_m \mathbf{B}_{nl}(\mathbf{u}_\beta) \mathbf{u}_\delta \mathbf{B}_{nl}(\mathbf{u}_\alpha) \mathbf{u}_\gamma \\ &+ \mathbf{A}_m \mathbf{B}_{nl}(\mathbf{u}_\gamma) \mathbf{u}_\delta \mathbf{B}_{nl}(\mathbf{u}_\alpha) \mathbf{u}_\beta) \end{aligned}$$

## REFERENCES

- [1] Patil, M.J., Hodges, D.H. and Cesnik, C.E., Characterizing the effects of geometrical nonlinearities on aeroelastic behavior of high-aspect ratio wings. In NASA Conference Publication, 1999 (pp. 501-510). NASA.
- [2] Patil, M.J. and Hodges, D.H., On the importance of aerodynamic and structural geometrical nonlinearities in aeroelastic behavior of high-aspect-ratio wings. *Journal of Fluids and Structures*, 2004, 19(7), pp.905-915.
- [3] Tang, D. and Dowell, E.H., Experimental and theoretical study on aeroelastic response of high-aspect-ratio wings. *AIAA journal*, 2001, 39(8), pp.1430-1441.
- [4] Avin, O., Raveh, D.E., Drachinsky, A., Ben-Shmuel, Y. and Tur, M., 2021. An experimental benchmark of a very flexible wing. In *AIAA Scitech 2021 Forum* (p. 1709).
- [5] Ritter, M., Hilger, J. and Zimmer, M., Static and dynamic simulations of the Pazy wing aeroelastic benchmark by nonlinear potential aerodynamics and detailed FE model. In *AIAA scitech 2021 forum* (p. 1713).
- [6] Riso, C. and Cesnik, C.E., Correlations between UM/NAST nonlinear aeroelastic simulations and the pre-Pazy wing experiment. In *AIAA Scitech 2021 Forum* (p. 1712).
- [7] Goizueta, N., Wynn, A., Palacios, R., Drachinsky, A. and Raveh, D.E. Flutter predictions for very flexible wing wind tunnel test. *Journal of Aircraft*, 59(4),2022, pp.1082-1097.
- [8] Drachinsky, A. and Raveh, D.E., 2022. Nonlinear aeroelastic analysis of highly flexible wings using the modal rotation method. *AIAA Journal*, 60(5), 2022, pp.3122-3134.
- [9] Riso, C. and Cesnik, C.E, Geometrically nonlinear effects in wing aeroelastic dynamics at large deflections. *Journal of Fluids and Structures*, 120, 2023, p.103897.
- [10] Cesnik, C. and Su, W., April. Nonlinear aeroelastic modeling and analysis of fully flexible aircraft. In *46th AIAA/ASME/ASCE/AHS/ASC Structures, Structural Dynamics and Materials Conference*, 2005 (p. 2169).
- [11] Ritter, M.R., An extended modal approach for nonlinear aeroelastic simulations of highly flexible aircraft structures. *Technische Universitaet Berlin (Germany)*, 2019.
- [12] Ritter, M., Cesnik, C.E. and Krüger, W.R., An enhanced modal approach for large deformation modeling of wing-like structures. In *56th AIAA/ASCE/AHS/ASC Structures, Structural Dynamics, and Materials Conference*, 2015 (p. 0176).
- [13] Drachinsky, A. and Raveh, D.E., Modal rotations: A modal-based method for large structural deformations of slender bodies. *AIAA Journal*, 58(7), 2020, pp.3159-3173.
- [14] Liang, K., A Koiter-Newton arclength method for buckling-sensitive structures. *Delft University of Technology*, 2013.
- [15] Sinha, K., Singh, N.K., Abdalla, M.M., De Breuker, R. and Alijani, F., A momentum subspace method for the model-order reduction in nonlinear structural dynamics: Theory and experiments. *International Journal of Non-Linear Mechanics*, 119, 2020, p.103314.



- [16] Sinha, K., Alijani, F., Krüger, W.R. and De Breuker, R., Koiter–Newton Based Model Reduction for Large Deflection Analysis of Wing Structures. *AIAA Journal*, 61(8), 2023, pp.3608-3617.
- [17] Sinha, K., Alijani, F., Krüger, W.R. and De Breuker, R., Nonlinear dynamics of wing-like structures using a momentum subspace-based Koiter-Newton reduction (*under review*)
- [18] Militello, C. and Felippa, C.A., The first ANDES elements: 9-dof plate bending triangles. *Computer methods in applied mechanics and engineering*, 93(2), 1991, pp.217-246.
- [19] Alvin, K., de La Fuente, H.M., Haugen, B. and Felippa, C.A., 1992. Membrane triangles with corner drilling freedoms—I. The EFF element. *Finite Elements in Analysis and Design*, 12(3-4), pp.163-187.
- [20] Newmark, N.M., A method of computation for structural dynamics. *Journal of the engineering mechanics division*, 85(3), 1959, pp.67-94.